Self-gravitating gaseous spheres in 5D framework

E. E. Kangal*[1]

[1] *Computer Technology and Information Systems,*
School of Applied Technology and Management of Erdemli,
Mersin University, Mersin-33740, Turkey

Abstract

One of the suitable theoretical idea for the polytrope in the Kaluza-Klein cosmology is discussed. Assuming a 5-dimensional (5D) spacetime model described by the Kaluza-Klein theory of gravity, we implement the energy density and pressure of the polytrope which is a self-gravitating gaseous sphere and still very useful as a crude approximation to more realistic stellar models. Next, we obtain the best-fit values of the auxiliary parameters given in the model according to the recent observational dataset. Finally, we study some cosmological features and the thermodynamical stability of the model.

PACS numbers: 04.50.+h, 95.35.+d, 98.80.-k

Keywords: Polytrope, dark energy, Kaluza-Klein, cosmology.

* evrimersin@gmail.com

I. INTRODUCTION

The cosmic harmony puzzle starts with the diminish of the adiabatic cold dark matter for structure formation[1]. Nearly two decades ago, astronomers figured out that the large scale structure growth in cold dark matter simulations supposed a shape parameter $\Upsilon \approx \Omega_m \eta \approx 0.25$ to generate molds which agree with the recent astrophysical data[2]. Hubble Space Telescope results[3], for $\eta \approx 0.7$, indicate a low density universe, i.e. $\Omega_m < 1$, excluding the Einstein-de Sitter type model. In addition to this, the predilection for inflation descriptions and the lower bound to the oldest globular clusters ages contributed to the implementation of the basic exigency of the cosmic harmony puzzle: $\Omega_m \approx 0.25$ and $\Omega_{de} = 1 - \Omega_m$[1, 4]. Subsequently, this picture was reinforced by many observations: observational dataset of SNe-Ia[5], CMB[6], LSS[7], WMAP[8–10], SDSS[11] and the Planck-2013, 2015 and 2018 results[12–14] indicate that the observable universe is at a speedy expansion phase which is imputed to dark constituents, which do not cluster as ordinary matters do and have negative large pressures.

Due to the dark content is not being detected directly, assuming the dominant components of the universe resemble familiar forms of matter or energy has not been justified yet. On the other hand, there are various theoretical candidates for the dark components of the universe in literature. The simplest proposal is the cosmological constant[15, 16], and its energy density ρ_Λ which remains constant in time and equation-of-state (EoS) parameter are given by

$$\rho_\Lambda = \frac{\Lambda}{8\pi G}, \qquad \omega = -1. \tag{1}$$

Unfortunately, this earliest dark energy candidate suffers from the famous cosmological constant issues such as the fine-tuning and cosmological coincidence. These issues have led many physicists to give different proposals for the dark contents puzzle. Therefore, there are two significant ways to investigate the current nature of the universe. The first one is to consider the modification of gravity (for a good review see Ref.[17] and references there in), and the second one is to assume the dark content territory of the universe (for a good review see Ref.[16] and references there in). It is noteworthy to emphasize here that the second method can also describe a non-minimal coupling case between the dark content and gravity to implement a scalar-tensor theory (see Ref.[19] for a good instance). The most notable one among various scalar field models is known as quintessence[18, 20] having an evolving scalar field ϕ with a self-interacting potential $V(\phi)$. Also, there are other dark content proposals, for instance, back-reaction definitions that assume the dark content as a back-reaction effect of inhomogeneities[21–23], Chaplygin gas[24, 25] and Polytrope[26, 27] models which unify the dark energy and the dark matter, and braneworld prescriptions, which interpret the speedy expansion era of the universe by formulating the general relativity in five dimensions[28].

A large number of theoretical physicist have been interested in higher dimensional field theory compactifications in order to interpret lower dimensional ones in a better new way. The most significant study among those is the compactification of the $6D(2,0)$-theory on a Riemann surface[29]. Subsequently, this work leads to various 4D super-conformal field theories. This notable construction can be considered to uncover many features of the 4D super-conformal ideas. For instance, it leads to Argyres-Seiberg type[30] duality which is manifested as diverse decomposition of the same Riemann surface[31]. Moreover, considering the existence of additional dimensions gives interesting conclusions to interpret the accelerated expansion behavior. The Kaluza-Klein theory including an interaction between electromagnetism and gravity is one of the most attractive ideas including additional dimension[32, 33]. The Kaluza-Klein theory of gravity is divided into two branches[34, 35]: the compact and non-compact ones. In the compact Kaluza-Klein theory, the additional fifth dimension is assumed to be length-like while, in the non-compact form, we have a mass-like fifth dimension. In fact, the non-compact version is a conclusion of the Campbell theorem in which one cannot assume any matter in a 5D manifold by hand[34, 35]. In subsequent studies, the original Kaluza-Klein theory of gravity becomes a basis of other higher dimensional proposals in various perspectives[36–45]. For a very useful review including higher dimensional ideas, one can check Ref.[46]. For a Kaluza-Klein type model to be able to understand the observed 4D world, it is indispensable for the additional dimensions to be compactified down to a size which one does not probe in particle physics experiments[47]. Appelquist and Chodos[48] showed that the main difference between the 5D Kaluza-Klein idea and other higher dimensional ($4+d$ with $d>1$) models is that the 5D field equations have a compactified classical solution. It is known that an energy-momentum tensor must be taken into account on the right-hand side of the Einstein field equation when the compactification is due to matter fields[47]. On the other hand, there are several redefinitions of original Chaplygin gas models (generalized[49–51], modified[52, 53], variable[54–58], variable generalized[59, 60], variable modified[61] and extended[62, 63] ones) and there is no a definite criterion to select one of them as capable of recent observations at all scales. Like the Chaplygin gas model, the polytrope gas describing self-gravitating gaseous spheres is also define a unified dark matter-energy scenario[26, 27, 64, 65].

One of the significant tasks in theoretical physics is to constrain the auxiliary parameters given in theoretical models. Investigating the luminosity distance measurements to a specific category of objects[66–72] is the most often considered way. Recently, a new technique including observational dataset of the Hubble parameter has been taken into account to test some cosmological proposals[73–84].

This paper is structured as following: in the next section, we exactly construct the five-dimensional form of the Polytropic model and discuss its adiabatic stability condition. In the third section, we use the recent observational dataset to constrain two free parameters of the five-dimensional Polytropic proposal. Next, in the fourth section, we study some physical features of the model in order to interpret it cosmologically. In the fifth section, we investigate the Polytropic cosmology via the generalized second law of thermodynamics. The last section is devoted to closing remarks. All numerical calculations and analyzes will be performed by using MATHEMATICA sofware[87].

II. KALUZA-KLEIN TYPE POLYTROPES

One of the most significant scalar field description for the role of dark energy is described by the following lagrangian density[88]

$$\pounds = V(\phi)\sqrt{1 + g^{\mu\nu}\partial_\mu\phi\partial_\nu\phi} \tag{2}$$

where ϕ denotes a scalar field function while $V(\phi)$ and $g^{\mu\nu}$ show a self-interacting potential and the inverse metric tensor, respectively. In a spatially flat Kaluza-Klein type Friedmann-Robertson-Walker space-time, the corresponding energy density and pressure of a tachyonic field are given, respectively, by

$$\rho_\phi = \frac{V(\phi)}{\sqrt{1-\dot{\phi}^2}}, \tag{3}$$

$$p_\phi = -V(\phi)\sqrt{1-\dot{\phi}^2}. \tag{4}$$

Additionally, the field equation for the scalar field is obtained as follows

$$\frac{\ddot{\phi}}{1-\dot{\phi}^2} + \frac{4\dot{a}\dot{\phi}}{a} + \frac{\partial_\phi V}{V} = 0. \tag{5}$$

A similar formulation, known as the tachyonic scalar field, can be written for a minimally coupled scalar field as

$$\rho_\phi = \frac{\dot{\phi}^2}{2} + V(\phi), \tag{6}$$

$$p_\phi = \frac{\dot{\phi}^2}{2} - V(\phi). \tag{7}$$

The tachyon scalar field model arising in the context of string theory[88, 89] has been intensively discussed recently in application to modern cosmology[90–97]. It can be easily concluded that the energy density and pressure given in equations (3), (4), (6) and (7) are related with the original Chaplygin gas[24, 25] state equation, i.e. $p = -\frac{B}{\rho}$, for the potential $V = B = constant$. Therefore, we see that the Chaplygin gas proposal coincides with the tachyonic field. The variable, generalized, modified or extended forms of the Chaplygin gas model describe a unified dark matter-energy scenario[49, 52–55, 62, 98]. Here, we consider another interesting proposal, which defines the polytropes[26, 27], and assumes that

$$p = \kappa \rho^{1+\frac{1}{m}}, \tag{8}$$

where both κ and m denote real constants. Additionally, m is called as the polytropic index. Note that, taking $m = -\frac{1}{2}$ with $\kappa = -B$ transforms this model into the original Chaplygin gas proposal. Moreover, assuming $m = -\frac{1}{\alpha+1}$ with $\kappa = -B$ reduces the relation (8) to the one, written for the generalized Chaplygin gas model[49–51].

The Kaluza-Klein type Friedmann-Robertson-Walker universe is described by the following line-element[99]

$$ds^2 = dt^2 - a^2(t)\left[\frac{dr^2}{1-kr^2} + r^2(d\theta^2 + \sin^2\theta d\varphi^2) + (1-kr^2)dx_5^2\right], \tag{9}$$

where k represents the curvature parameter. Here, we have $k = -1$, $k = 0$ and $k = +1$ for the closed, flat and open universes, respectively. The recent observational data[5, 8, 11, 13, 100] strongly indicate a spatially flat universe, from this point of view we take $k = 0$ in further calculations. Next, we suppose that the Kaluza-Klein type Friedmann-Robertson-Walker universe is dominated by the Polytrope that is described by the following relation

$$T_{\mu\nu} = (\rho + p)u_\mu u_\nu - g_{\mu\nu}p \tag{10}$$

with u_μ defining the five-velocity vector.

Consequently, the Kaluza-Klein forms of Friedmann equations are found as

$$H^2 = \frac{4\pi G}{3}\rho, \tag{11}$$

$$2H^2 + \dot{H} = -\frac{8\pi G}{3}p, \tag{12}$$

where the over-dot implies a time-derivative and $H = \frac{\dot{a}}{a}$ indicates the Hubble parameter. Note that, for simplicity, we assume $\frac{4\pi G}{3} = 1$ in further calculations. In the Kaluza-Klein framework, we get

$$\dot{\rho} + 4H(1+\omega)\rho = 0, \tag{13}$$

with the fact that the corresponding Polytropic EoS parameter is defined as $\omega = \frac{p}{\rho}$. One can find that the above relation can be transformed to an elegant form

$$d(\rho a^4) + pd(a^4) = 0. \tag{14}$$

One can integrate this equation and show that the Polytropic energy density evolves as

$$\rho = \frac{1}{a^4}\left(\frac{4\kappa}{m}\int a^{-1-\frac{4}{m}}da + c\right)^{-m}. \tag{15}$$

In the above result, c denotes a constant. Subsequently, solving explicitly the above equation gives

$$\rho = \left[c\sqrt[m]{a^4} - \kappa\right]^{-m}. \tag{16}$$

We know that the cosmological and present energy densities are related with each other, i.e. $\rho_{pre} = 1.3\rho_{cos}$[62]. Consequently, the constant c may be written in terms of a_0 which is the present cosmic scale factor value. For convenience, we further assume that $a_0 = 1$. Thus, it follows that $c = \sqrt[-m]{1.3} + \kappa$. Now, we define a new parameter $\xi = \frac{c}{c-\kappa}$, then it transforms equation (16) into another convenient relation as

$$\rho = \sqrt[-\frac{1}{m}]{(c-\kappa)(1-\xi+\xi a^{\frac{4}{m}})}. \tag{17}$$

Making use of the red shift parameter z in cosmological calculations helps us to fix auxiliary parameters. It is well known that $z = \frac{1}{a} - 1$. Hence, we can write

$$H(z) = -\frac{\dot{z}}{1+z}. \tag{18}$$

Moreover, we can discuss density perturbations in order to investigate the instability conditions of the Polytropic proposal by making use of the following relations[101]

$$\tilde{g}_{\mu\nu} = g_{\mu\nu} + h_{\mu\nu}, \qquad \tilde{u}_\mu = u_\mu + \delta u_\mu, \tag{19}$$

$$\tilde{\rho}_\mu = \rho_\mu + \delta\rho_\mu, \qquad \tilde{p}_\mu = p_\mu + \delta p_\mu, \tag{20}$$

where $h_{\mu\nu}$, δu_μ, $\delta\rho_\mu$ and δp_μ represent small perturbations around $g_{\mu\nu}$, u_μ, ρ_μ and p_μ, respectively. Thus, the evolution of the perturbational case can be defined by the following newtonian relation[101]

$$\ddot{\delta} - \frac{2\dot{z}}{1+z}\dot{\delta} + \left[\lambda^2(z+1)^2\vartheta_s^2 + \frac{3}{z+1}\left(\frac{2\dot{z}}{z+1} - \ddot{z}\right)\right]\delta = 0, \tag{21}$$

where $\delta = \frac{\delta\rho}{\rho}$. Additionally, λ and ϑ_s show the wavelength of the perturbations and the speed of sound, respectively. It is known that the speed of sound can be calculated by using

$$\vartheta_s^2 = \frac{\partial p}{\partial \rho} = \frac{\dot{p}}{\dot{\rho}} = \frac{p'}{\rho'}, \tag{22}$$

where the prime represents derivative with respect to z. Now, performing required computations yields

$$\vartheta_s^2 = \left[1 + (1+z)^{-\frac{4}{m}}\left(\frac{0.43}{\kappa} + 1\right)\right], \tag{23}$$

which is indicating that ϑ_s^2 remains always positive if we have $\kappa > -2.3$. Therefore, under this case, there is no concern about imaginary sound speed or instability of the selected proposal. In FIG. 1, we plot the $\vartheta_s^2 \sim z$ relation by taking the corresponding free parameters as $\kappa = -0.5$, $m = -2.4$ (blue dashed line) and $m = 2.4$ (red line). One can conclude that $\vartheta_s^2 \geq 0$ without any restriction as we mentioned in the above text. It is known that negative values of ϑ_s^2 may lead us to some problematic issues. For instance, if there is no interaction between gravity and a fluid, negative ϑ_s^2 values imply an instable case under density perturbations. It can be seen from the FIG. 1 that the squared adiabatic sound speed always has positive values, which means the Polytropic model is stable throughout the history of the universe.

III. FITTING THE MODEL WITH RECENT OBSERVATIONAL DATASET

Furthermore, using the relation $E(z) \equiv \frac{H(z)}{H_0}$ where H_0 indicates the recent observational value of the Hubble parameter, we find

$$H(z) = H_0\left[(c-\kappa)(1 - \xi + \xi(1+z)^{-\frac{4}{m}})\right]^{-\frac{m}{2}}. \tag{24}$$

Accordingly, there are two auxiliary parameters in the Polytropic description: κ and m. Now, considering some observable $H(z)$ data[102–115], we further focus on the validity of

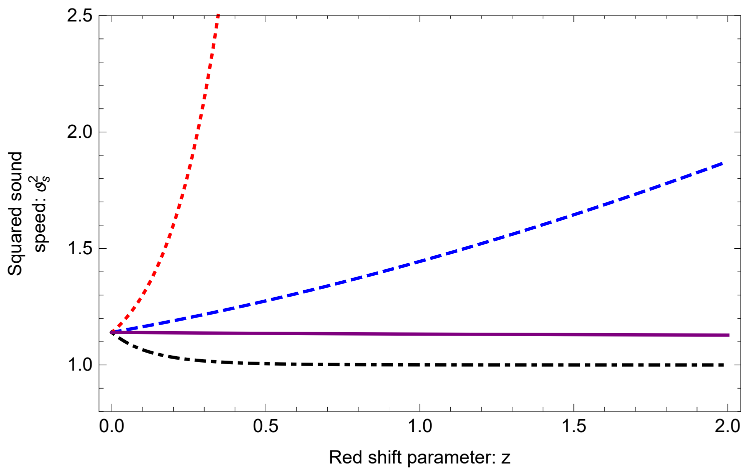

FIG. 1: $\vartheta_s^2 \sim z$ relation with auxiliary parameters $\kappa = -0.5$, $m = -2.4$ (blue dashed line), $m = -0.5$ (red dotted line), $m = 0.5$ (black dot-dashed line) and $m = 50$ (purple solid line).

the constraints on the auxiliary parameters given in the Polytropic model. In TABLE I, we use the currently available observational $H(z)$ data[102]. Here, DGA and RBAO represent the Differential Galactic Age and the Radial Baryonic Acoustic Oscillation techniques, respectively.

In FIG. 2, we have depicted the $m \sim \kappa$ phase space by making use of the observational values of the Hubble parameter given in TABLE I. While performing this analysis, we put the experimental results into the theoretical proposal given in the equation (24) in order to get the best-fit values of the auxiliary parameters. One can see that we have an intensive mesh zone in the bottom left side of the plot. Additionally, we also conclude that there is an exclusion zone for the (m, κ)-pair in the upper right side of the plot.

On the other hand, one can reach the best-fit values also by employing the standard minimization of χ^2 written as

$$\chi^2 = \sum_i \frac{[H_{theo}(\vec{s}|z_i) - H_{obs}(z_i)]^2}{\sigma^2(z_i)} \tag{25}$$

where $H_{theo}(\vec{s}|z_i)$ shows the theoretical Hubble parameter at red shift z_i defined by the relation (24), $\vec{s} = (H_0, \kappa, m)$ is the set of free parameters, $H_{obs}(\vec{s}|z_i)$ gives the observational $H(z)$ dataset and $\sigma^2(z_i)$ represent the uncertainty of each $H_{obs}(\vec{s}|z_i)$.

Our main target is just to obtain the primary trends in the fits by selecting suitable values of the set $\vec{s}$. The best-fit values are $H_0 = 67.8 \pm 0.9$ km s^{-1} Mpc^{-1}[13], $\kappa = -0.5$ and $m = -2.4$. In FIG. 3, we analyze the confidence control parameter χ^2 as a function of the

TABLE I: The current observational dataset for $H(z)$ [102].

z	H	Technique	Reference
0.0708	69.00∓19.68	DGA	Zhang et al.[103]
0.1200	68.60∓26.20	DGA	Zhang et al.[103]
0.1700	83.00∓8.000	DGA	Simon, Verde and Jimenez[104]
0.1990	75.00∓5.000	DGA	Moresco et al.[105]
0.2400	79.69∓2.650	RBAO	Gaztañaga, Cabré and Hui[106]
0.2800	88.80∓36.60	DGA	Zhang et al.[103]
0.3500	84.40∓7.000	RBAO	Xu et al.[107]
0.3802	83.00∓13.50	DGA	Moresco et al.[105]
0.4000	95.00∓17.00	DGA	Simon, Verde and Jimenez[104]
0.4247	87.10∓11.20	DGA	Moresco et al.[108]
0.4300	86.45∓3.680	RBAO	Gaztañaga, Cabré and Hui[106]
0.4497	92.80∓12.90	DGA	Moresco et al.[108]
0.4783	80.90∓9.000	DGA	Moresco et al.[108]
0.4800	97.00∓62.00	DGA	Stern et al.[109], Jimenez et al.[110]
0.5700	92.40∓4.500	RBAO	Samushia et al.[111]
0.5930	104.0∓13.00	DGA	Moresco et al.[105]
0.6800	92.00∓8.000	DGA	Moresco et al.[105]
0.7300	97.30∓7.000	RBAO	Blake et al.[112]
0.7810	105.0∓12.00	DGA	Moresco et al.[105]
0.8750	125.0∓17.50	DGA	Moresco et al.[105]
0.9000	117.0∓23.00	DGA	Simon, Verde and Jimenez[104]
1.3000	168.0∓17.00	DGA	Farooq and Ratra[113]
1.4300	177.0∓18.00	DGA	Farooq and Ratra[113]
1.5300	140.0∓14.00	DGA	Simon, Verde and Jimenez[104]
1.7500	202.0∓40.00	DGA	Thakur et al.[114]
1.9650	186.5∓50.40	DGA	Moresco et al.[105]
2.3400	222.0∓7.000	RBAO	Delubac et al.[115]

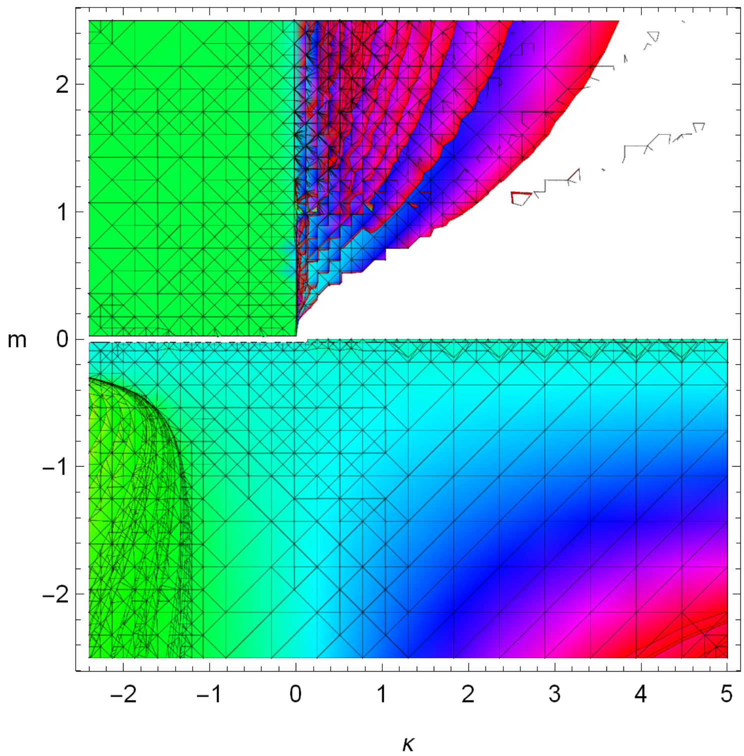

FIG. 2: The $m \sim \kappa$ phase space according to the observational dataset given in TABLE I.

red shift in the 1σ, 2σ and 3σ confidence regions.

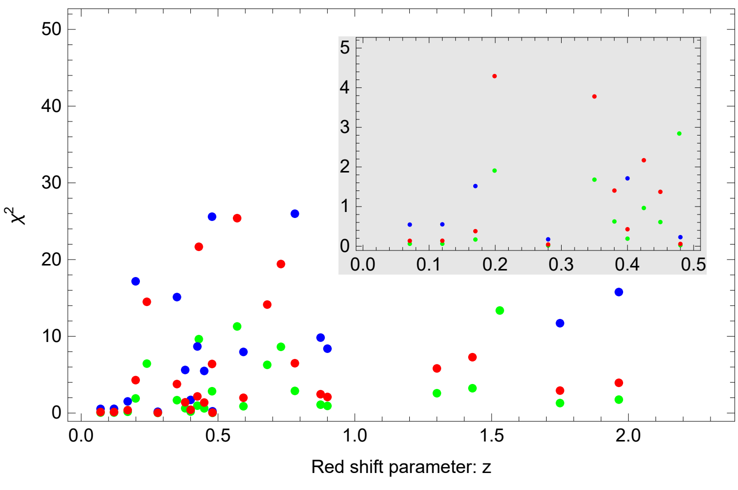

FIG. 3: The corresponding values of the confidence control parameter χ^2 with auxiliary parameters $\kappa = -0.5$ and $m = -2.4$ in the 1σ (blue dots), 2σ (red dots) and 3σ (green dots) confidence regions.

FIG. 4 gives the evolutionary nature of the Hubble parameter in the 1σ confidence region. Note that, in FIG. 4, the circles indicate the recent observable values.

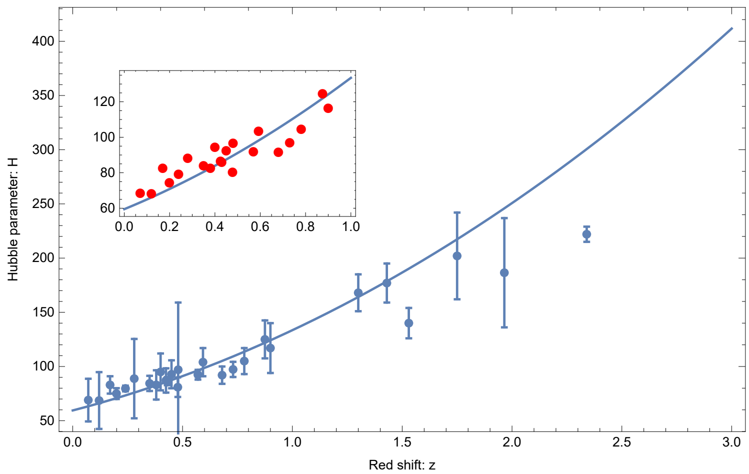

FIG. 4: $H \sim z$ relation with free parameters $\kappa = -0.5$ and $m = -2.4$ in the 1σ confidence region.

IV. COSMOLOGICAL FEATURES

A. Polytropic EoS parameter

Next, using equations (8) and (16), the corresponding EoS parameter, describing a self-gravitating Polytropic gaseous sphere, is found as

$$\omega = (\xi - 1)\left[1 - \xi + \xi(1+z)^{-\frac{4}{m}}\right]^{-1}. \tag{26}$$

In FIG. 5, we have depicted the evolution of the EoS parameter as a function of the cosmic time. To perform a meaningful analysis, we also assume three different scale factor cases: (i) the blue dashed line indicates the late-time acceleration case, i.e. $z = \frac{1}{t^2} - 1$, (ii) the black dotted line shows the matter dominated solution, i.e. $z = \frac{1}{t^{\frac{2}{3}}} - 1$ and (iii) the red solid line represents the radiation dominated model, i.e. $z = \frac{1}{\sqrt{t}} - 1$. In three of the cases, it can be seen that the EoS parameter cannot cross -1 line. From FIG. 4, one can conclude that the 5D form of Polytropic EoS parameter behaves like quintessence energy, i.e. $\omega > -1$. The ΛCDM model is one of the most common description to understand the acceleration feature of our universe. It is dominated by the cold dark matter with the EoS $\omega = 0$ and the cosmological constant Λ with $\omega = -1$. Hence, it may be concluded that, at late times, the 5D Polytropic model agrees with the ΛCDM cosmology.

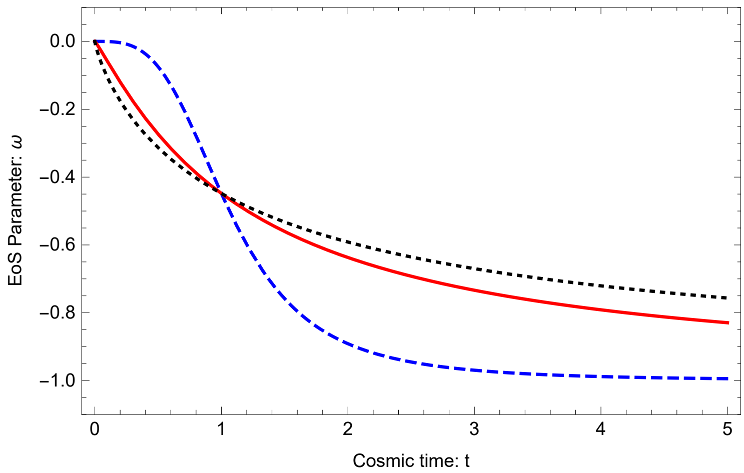

FIG. 5: Relation between the EoS parameter ω and the cosmic time t with $\kappa = -0.5$ and $m = -2.4$.

B. Deceleration parameter

Making use of the relation $q = -\frac{\ddot{a}}{aH^2}$ with the equation (26) leads us to the following conclusion

$$q \approx -1 + \frac{3\xi}{2(1-\xi)^2}(1+z)^{-\frac{4}{m}}, \tag{27}$$

where the free parameters ξ and m have prominent influences. So, we must have $\frac{3\xi}{2(1-\xi)^2} < 0$, otherwise we may get positive values for q. See the $q \sim t$ relation for $\xi = -0.5$ and $m = -2.4$ in FIG. 6. Here, the blue dashed line denotes the late-time acceleration solution, the black dotted line is the matter dominated definition and the red solid line shows the radiation dominated model. The deceleration parameter initially has a positive value in three of the cases, then the universe enters into the accelerating expansion phase, and finally the deceleration parameter reaches $q = -1$ at the end of the universe.

C. Statefinder Diagnostic

The EoS parameter of some geometrical models obtained by modifying the gravitational part of the general relativistic field equations does no longer play a requisite role. Thus, another diagnosis is essential to discriminate the model among different theoretical descriptions. In order to reach this aim, Sahni et. al[117] introduced (r, s) parameters which are known as the statefinders. Trajectories in the statefinders-plane imply qualitatively different features[102, 118–121]. For instance, the ΛCDM model includes a fixed point $(r, s) \equiv (1, 0)$.

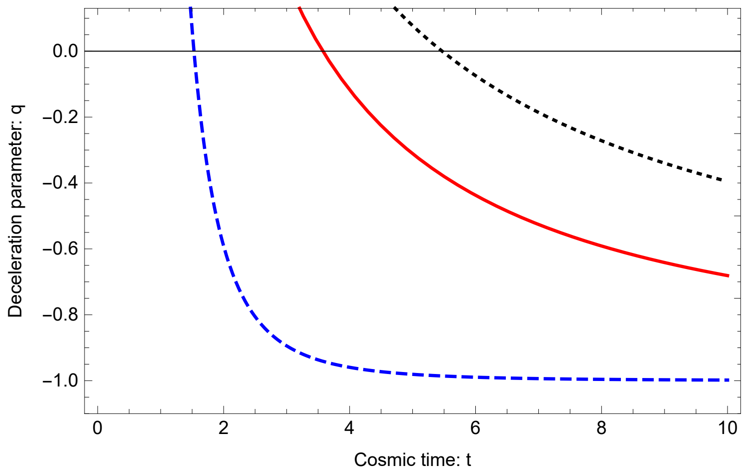

FIG. 6: Relation between the deceleration parameter q and the cosmic time t with $\kappa = -0.5$ and $m = -2.4$.

Next, we have $(r, s) \equiv (1, 1)$ and $(r, s) \equiv (\infty, -\infty)$ for the standard cold dark matter and the Einstein static universe models, respectively[122].

The statefinders pair is basically defined as

$$r = \frac{\ddot{a}}{aH^3}, \tag{28}$$

$$s = \frac{r-1}{3(q-\frac{1}{2})}. \tag{29}$$

It is possible to re-write the expression of r in a more convenient form as follows

$$r = q + 2q^2 + (1+z)q', \tag{30}$$

Making use of equations (28), (29) and (30), we find

$$\frac{r}{3} = 1 + \frac{5c(\xi-1)}{\xi}\frac{1}{f} + 2c(\xi-1)\left[\frac{3c(\xi-1)}{\xi^2} + \frac{(1+z)^{-\frac{4}{m}}}{m}\right]\frac{1}{f^2}, \tag{31}$$

$$3s = \frac{2 + \frac{15c(\xi-1)}{\xi}\frac{1}{f} + 6c(\xi-1)\left[\frac{3c(\xi-1)}{\xi^2} + \frac{(1+z)^{-\frac{4}{m}}}{m}\right]\frac{1}{f^2}}{\frac{1}{2} - \frac{3c(\xi-1)}{\xi}\frac{1}{f}}, \tag{32}$$

where

$$f = 1 - \xi + \xi(1+z)^{-\frac{4}{m}}. \tag{33}$$

In FIG. 7, we plot the (r, s)-plane for the five-dimensional Polytropic model. It can be seen that r and s parameters first decrease from some negative values, then start to increase from some other negative values to the ΛCDM fixed point $(r, s) \equiv (1, 0)$ and after that continue to increase.

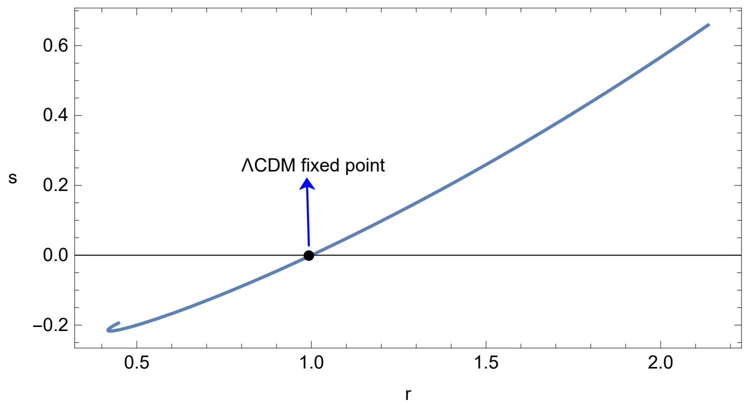

FIG. 7: $r \sim z$ (dashed blue line) and $s \sim z$ (dotted red line) relations with auxiliary parameters $\kappa = -0.5$ and $m = -2.4$.

D. Neo-classical behavior

It is significant to implement a causality connection between source and observer at any time. We can compute the proper distance by making use of the following relation[123]

$$d(a) = \int_1^a \frac{da}{a\dot{a}} \tag{34}$$

For the Polytropic model, it gives us the following result

$$d(a) = \frac{(-\kappa)^{\frac{m}{2}}}{a} {}_2F_1 \left[-\frac{m}{2}, -\frac{m}{4}, 1 - \frac{m}{4}, \frac{ca^{\frac{4}{m}}}{\kappa} \right] \tag{35}$$

where ${}_2F_1$ is the Kummer Confluent Hypergeometric function of the second kind and it is given by

$${}_2F_1[K, L, M; x] = 1 + \frac{KL}{x} + \frac{K(K+1)L(L+1)}{M(M+1)} \frac{x^2}{2!} + ... = \sum_{i=1}^{\infty} \frac{K_i L_i}{M_i} \frac{x^i}{i!} \tag{36}$$

with $c \neq 0, -1, -2, ...$ and $|x| < 1$.

On the other hand, the luminosity distance d_L is another significant neo-classical quantity which is helping us to calculate the distribution of light. Making use of the total energy L emitted by a source per unit time and l indicating the apparent luminosity of an object, the luminosity distance is given by[123] $d_L = \sqrt{\frac{L}{4\pi l}}$. Thus, it can be found[123] that $d_L = (1+z)d(z)$. Using this description, one can calculate the following result for the Polytropic model

$$d_L = (-\kappa)^{\frac{m}{2}} (1+z)^2 {}_2F_1 \left[-\frac{m}{2}, -\frac{m}{4}, 1 - \frac{m}{4}, \frac{c(1+z)^{-\frac{4}{m}}}{\kappa} \right]. \tag{37}$$

We see that the proper distance $d(z)$ and the luminosity distance d_L depend upon the cosmic red shift parameter and both of them are also increasing functions of z. In FIG. 8, plot $d(z) \sim z$ and $d_L \sim z$ relations.

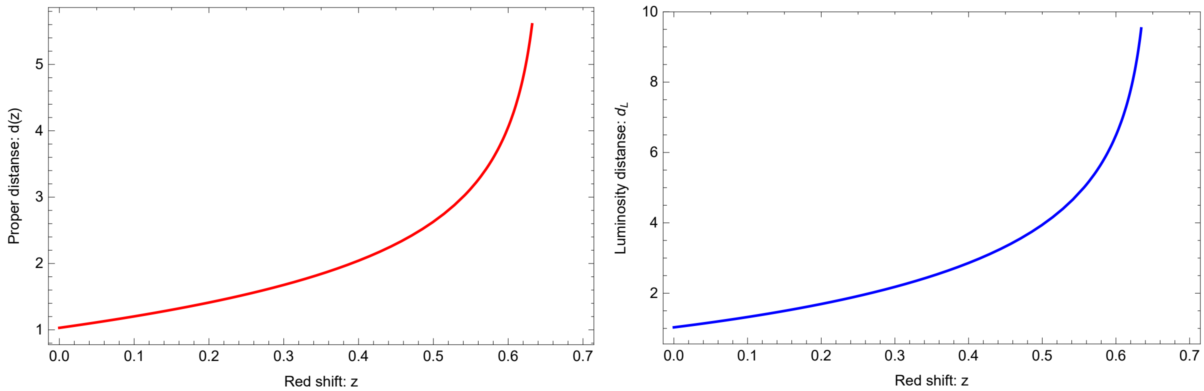

FIG. 8: Numerical analysis of the proper distance $d(z)$ and the luminosity distance d_L with auxiliary parameters $\kappa = -0.5$ and $m = -2.4$.

E. Scaling case

The evolution of the Polytropic model is equivalent to a dark matter-energy coupling which is described by the EoS parameter $\omega = (\xi - 1)\left[1 - \xi + \xi(1+z)^{-\frac{4}{m}}\right]^{-1}$. Assuming a scaling condition, i.e. $\rho = \rho_m + \rho_e$ with $\rho_e \propto \rho_m(1+z)^{\frac{4}{m}}$, in the Polytropic framework leads to

$$\rho_m + \rho_e = \rho_{cr} \sqrt[-\frac{1}{m}]{(1 - \Omega_m^0) + \Omega_m^0(1+z)^{-\frac{4}{m}}}. \tag{38}$$

In the above relation, ρ_{cr} is a constant and represents the critical energy density while Ω_m^0 indicates the matter density parameter. After focusing on equations (17) and (38), we see that ξ can be taken into account as an effective matter density Ω_m^0. If the coupled conditions is defined by

$$\dot{\rho}_m + 4H\rho_m = \Xi, \tag{39}$$

$$\dot{\rho}_e + 4H\left[1 + (\xi - 1)\left[1 - \xi + \xi(1+z)^{-\frac{4}{m}}\right]^{-1}\right]\rho_e = -\Xi, \tag{40}$$

then the interaction term can be characterized by[116]

$$\Xi = \frac{4H\rho_m\rho_e}{\rho_e + \rho_m}\frac{\xi - 1}{1 - \xi + \xi(1+z)^{-\frac{4}{m}}}, \tag{41}$$

which gives the interaction between the dark matter and the dark energy. From this point of view, one can conclude that the background evolution of the Polytropic model is identical to an interacting case. It is important to mention here that negative Ξ values indicate energy transition to the dark energy territory, and positive values of Ξ imply the vice versa condition. Recently, the Cluster Abell A586[124, 125] has observed this interesting event, however its importance has not been clarified yet.

V. THERMODYNAMICAL STABILITY

In this part of the work, we focus on the thermodynamical features of the Polytropic gaseous sphere description leading to the discussion of the *generalized* second law of thermodynamics, i.e. $T\dot{S}_{tot}(t) \geq 0$ or $TS'_{tot} \leq 0$ where T shows the temperature, S_{tot} describes the total entropy and the prime indicates derivative with respect to the red shift z. Note that we can write $\frac{d}{dt} = -(1+z)H\frac{d}{dz}$. To reach this goal, the flat Kaluza-Klein universe is assumed to be a thermodynamical system. In a flat framework, the apparent horizon is identical to the Hubble horizon[126–128]:

$$r_a = \lim_{k\to 0}\left[H^2 + k(1+z)^2\right]^{-\frac{1}{2}} = \frac{1}{H}. \tag{42}$$

Additionally, the temperature T and the horizon entropy S are given as follows

$$T = \frac{1}{2\pi r_a} = \frac{H}{2\pi}, \qquad S_h = \frac{A}{4G}, \tag{43}$$

where $A = 2\pi^2 r_a^3$ is the surface area of 4-sphere. Hence, we get[42]

$$S_h = \frac{\pi^2}{2G}\frac{1}{H^3}, \tag{44}$$

Next, the internal entropy is written as[129]

$$TdS_i = pdV + dE_i, \tag{45}$$

which is known as the Gibbs' formulation. In the above expression, S_i, $E_i = \rho V$ and $V = \frac{1}{2}\pi^2 r_a^4$ indicate the internal entropy, internal energy and the additional-dimensional volume, respectively.

After performing a time derivation in the relation (45) and making use of the equation (13) or (14), one can find that

$$T\dot{S}_i = (\rho + p)(\dot{V} - 4HV), \tag{46}$$

and substituting relations (11) and (12) into the above equation gives

$$TS_i' = -\frac{\pi^2 H'}{H^4}[(1+z)H' + H]. \tag{47}$$

On the other hand, using the relations given in (43), the evolution of the horizon entropy in a flat Kaluza-Klein type spacetime is calculated as

$$TS_h' = -\frac{\pi^2 H'}{H^3}. \tag{48}$$

At this step, we can now focus on the second thermodynamical law. Adding equations (47) and (48), we can get the total entropy associated with the flat Kaluza-Klein universe dominated by the Polytropic gas. Thus, it can be found that

$$TS_{tot}' = T(S_i' + S_h') = -\frac{\pi^2 H'}{H^4}\left[(1+z)H' + 2H\right]. \tag{49}$$

Consequently, substituting the relation (24) into the above relation leads us to the following result

$$TS_{tot}' = -\frac{4\pi^2}{H^2} g(g+1), \tag{50}$$

where

$$g(z) = \frac{\xi(1+z)^{-1}}{\xi + (1-\xi)\sqrt[m]{(1+z)^4}}. \tag{51}$$

We have plotted the relation $TS_{tot}' \sim z$ in FIG. 9. It can be seen that the generalized second law of thermodynamics is valid for the Polytropic gas dominating the Kaluza-Klein universe at all times.

VI. CLOSING REMARKS

The dynamical nature of a Polytropic type unified dark matter-energy scenario has been investigated in the 5D Kaluza-Klein framework and it is concluded that this model may have the ability to explain the speedy expansion phase of our universe.

As a first step, we compute theoretical energy density and Hubble parameter relations. Besides, the adiabatic stability condition of the proposal has been also discussed by focusing on the speed of sound, and we have seen that there is no concern about the instable feature of the model, if one consider the meaningful values of κ. Next, we have fitted data from the recent observations to fix the free parameters m and κ given in the model. Moreover, considering our calculations, we have discussed some physical features of the model and confirm

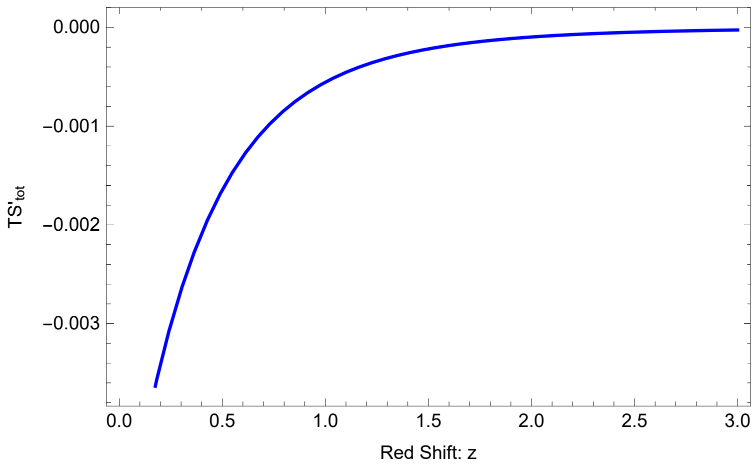

FIG. 9: The evolution of TS'_{tot} in terms of the red shift parameter z for the case with $\kappa = -0.5$ and $m = -2.4$.

that the second thermodynamical law is satisfied, which means the theoretical description may be stabilized by assuming best-fit values of the free parameters m and κ.

In summary, the scenario of the Polytropic dark content is compatible with recent observations.

Acknowledgments

This study was supported linguistically by the Technology Transfer Office Academic Writing Center of Mersin University.

---

[1] J.P. Ostriker and P.J. Steinhardt, Nature 377 (1995) 600.

[2] R. Cen and J.P. Ostriker, Astrophys. J. 538 (2000) 83.

[3] W.L. Freedman, et al., Nature 371 (1994) 757; Astrophys. J. 55 (2001) 47.

[4] A.L.B. Ribeiro and A.C. Schilling, Astrophys. Space Sci. 321 (2009) 43.

[5] S. Perlmutter, et al., Nature 391 (1998) 51; Astrophys. J. 517 (1999) 565.

[6] A.D. Miller, et al., Astrophys. J. Lett. 524 (1999) L1.

[7] N.A. Bahcall, J.P. Ostriker, S. Perlmutter and P.J. Steinhardt, Science 284 (1999) 1481.

[8] C.L. Bennett, et al., Astrophys. J. Suppl. 148 (2003) 1.

[9] S.L. Brile, O. Lahav, J.P. Ostriker and P.J. Steinhardt, Science 299 (2003) 1532.

[10] D.N. Spergel, et al., The Astrophysical Journal Supplement Series 148 (2003) 175.

[11] M. Tegmark, et al., Phys. Rev. D 69 (2004) 103501.

[12] Planck Collaboration (P.A.R. Ade, et al.), A&A 571 (2014) A16.

[13] Planck Collaboration (P.A.R. Ade, et al.), A&A 594 (2016) A13.

[14] Planck Collaboration (N. Aghanim, et al.), e-Print: 1807.06209.

[15] V. Sahni and A. Starobinsky, Int. J. Mod. Phys. D 9 (2000) 373.

[16] E.J. Copeland, M. Sami and S. Tsujikawa, Int. J. Mod. Phys. D 15 (2006) 1753.

[17] S. Nojiri and S.D. Odintsov, Int. J. Geom. Methods Mod. 4 (2007) 115.

[18] B. Ratra and P.J.E. Peebles, Phys. Rev. D 37 (1988) 3406.

[19] S. Nojiri and S.D. Odintsov, Phys. Lett. B 631 (2005) 1.

[20] P.J.E. Peebles and B. Ratra, ApJ 325 (1988) L17.

[21] T. Buchert, Gen. Rel. Gravit. 32 (2000) 105.

[22] S. Rösönen, J. Cosmol. Astropart. Phys. 2 (2004) 003.

[23] E. W. Kolb, S. Matarrese and A. Riotto, New Journal of Physics 8 (2006) 322.

[24] A. Yu. Kamenshchik, U. Moschella and V. Pasquier, Phys. Lett. B 511 (2001) 265.

[25] M. C. Bento, O. Bertolami and A. A. Sen, Phys. Rev. D 66 (2002) 043507.

[26] S. Chandrasekhar, "An Introduction to the Study of Stellar Structure", (1939, Dover editions: 1958, 1967)

[27] J. Christensen-Dalsgard, "Lecture Notes on Stellar Structure and Evolution", (Aarhus Univ. Press, Aarhus, (2004) p.13.

[28] C. Cséki, M. Graesser, L. Randall and J. Terning, Phys. Rev. D 62 (2000) 045015.

[29] D. Gaiotto, JHEP 1208 (2012) 034.

[30] P.C. Argyres and N. Seiberg, JHEP 0712 (2007) 088.

[31] G. Zafrir, JHEP 01 (2017) 097.

[32] T. Kaluza, Sits. Press. Akad. Wiss. Math. Phys. K 1 (1921) 895.

[33] O. Klein, Zeits. Phys. 37 (1926) 895.

[34] M. Bellini, Nucl. Phys. B 660 (2003) 389.

[35] P.S. Wesson, Gen. Rel. Gravit. 16 (1984) 193.

[36] J. Clifford, "D-Branes", Cambridge Univ. Press, Cambridge (2003).

[37] J. Polchinski, "String Theory", Cambridge Univ. Press, Cambridge (1998).

[38] J. Wess and J. Bagger, "Supersymmetry and Supergravity", Princeton Univ. Press, Princeton

(1992).

[39] M. Salti, H. Yanar, O. Aydogdu and K. Sogut, Astrophys. Space Sci. 362 (2017) 207.

[40] S. Erkan, N. Pirinccioglu, M. Salti and O. Aydogdu, Eur. Phys. J. Plus 132 (2017) 536.

[41] M. Salti, O. Aydogdu, A. Tas, K. Sogut and E. E. Kangal, Can. J. Phys. (2018) In press.

[42] M. Salti, O. Aydogdu, H. Yanar and K. Sogut, Annals Phys. 390 (2018) 131.

[43] A.I. Keskin and I. Acikgoz, Astrophys. Space Sci. 361 (2016) 391.

[44] A.I. Keskin, Astrophys. Space Sci. 362 (2017) 50.

[45] A.I. Keskin, Int. J. Mod. Phys. D 27 (2018) 1850078.

[46] J.M. Overduin and P.S. Wesson, Phys. Rep. 283 (1997) 303.

[47] D. Bailin and A. Love, Rep. Prog. Phys. 50 (1987) 1087.

[48] T. Appelquist and A. Chodos, Phys. Rev. Lett. 50 (1983) 141; Phys. Rev. D 28 (1983) 772.

[49] N. Bilic, G.B. Tupper, and R.D. Viollier, Phys. Lett. B 535 (2002) 17.

[50] H. Saadat and B. Pourhassan, Int. J. Theor. Phys. 53 (2014) 1168.

[51] X.-H. Zhai, Y.-D. Xu and X.-Z. Li, Int. J. Mod. Phys. D 15 (2006) 1151.

[52] U. Debnath, A. Banerjee, and S. Chakraborty, Class. Quant. Grav. 21 (2004) 5609.

[53] J. Naji, B. Pourhassan and A.R. Amani, Int. J. Mod. Phys. D 23 (2013) 1450020.

[54] L.P. Chimento and A.S. Jakubi, Int. J. Mod. Phys. D 5 (1996) 71.

[55] T. Matos, F.S. Guzman and L.A. Urena-Lopez, Class. Quant. Grav. 17 (2000) 1707.

[56] L.A. Urena-Lopez and T. Matos, Phys. Rev. D 62 (2000) 081302.

[57] A. Gonzales, T. Matos and I. Quiros, Phys. Rev. D 71 (2005) 084029.

[58] Z.-K. Guo and Y.-Z. Zhang, Phys. Lett. B 645 (2007) 326.

[59] J. Lu, Phys. Lett. B 680 (2009) 404.

[60] D. Panigrahi and S. Chatterjee, JCAP 05 (2016) 052.

[61] D. Panigrahi and S. Chatterjee, Gen. Rel. Grav. 49 (2017) 35.

[62] E.O. Kahya, M. Khurshudyan, B. Pourhassan, R. Myrzakulov and A. Pasqua, Eur. Phys. J. C 75 (2015) 43.

[63] E.O. Kahya and B. Pourhassan, Astrophys. Space Sci. 353 (2014) 677.

[64] M. Askin, M. Salti and O. Aydogdu, Mod. Phys. Lett. A 32 (2017) 1750177.

[65] M. Salti, I. Acikgoz and H. Abedi, Chin. J. Phys. 52 (2014) 939.

[66] S.M. Carroll, E. Farhi and A. H. Guth, MIT preprint CTP-2117, hep-th/9207037.

[67] S. Nesseris and L. Perivolaropoulos, Phys. Rev. D 70 (2004) 043531.

[68] Z. G. Dai, E. W. Liang and D. Xu, Ap. J. Lett. 612 (2004) L101.

[69] Z. H. Zhu, M. K. Fujimoto and X. T. He, Astron. Astrophys. 417 (2004) 833.

[70] D.J. Eisenstein, et al., Ap. J. 633 (2005) 560.

[71] Y. Wang and P. Mukherjee, Ap. J. 650(2006) 1.

[72] D.N. Spergel et al., Astrophys. J. Suppl. 170 (2007) 377.

[73] Z.-L. Yi and T.-J. Zhang, Mod. Phys. Lett. A 22 (2007) 41.

[74] L. Samushia and B. Ratra, Ap. J. Lett. 650 (2006) L5.

[75] J.F. Zhang, X. Zhang and H.Y. Liu, Eur. Phys. J. C 52 (2007) 693.

[76] H. Wei and S.N. Zhang, Phys. Rev. D 76 (2007) 063003.

[77] X. Zhang and F.Q. Wu, Phys. Rev. D 76 (2007) 023502.

[78] M.A. Dantas, J.S. Alcaniz, D. Jain and A. Dev, Astron. Astrophys. 467 (2007) 421.

[79] P.X. Wu and H.W. Yu, Phys. Lett. B 644 (2007) 16.

[80] H. Lin, et al., Mod. Phys. Lett. A 24 (2009) 1699.

[81] H. Saadat and B. Pourhassan, Int. J. Theor. Phys. 52 (2013) 3712.

[82] H. Saadat and B. Pourhassan, Int. J. Theor. Phys. 52 (2013) 1309.

[83] Ali R. Amani and B. Pourhassan, Int. J. of Geometric Methods in Modern Physics 11 (2014) 1450065.

[84] H. Saadat and B. Pourhassan, Astrophys. Space Sci. 343 (2013) 783.

[85] J. Sadeghi, B. Pourhassan, M. Khurshudyan and H. Farahani, Int. J. Theor. Phys. 53 (2014) 911.

[86] B. Pourhassan, Int. J. Mod. Phys. D 22 (2013) 1350061.

[87] Wolfram Research Inc., Wolfram Mathematica 9.0, 2012.

[88] M.R. Gaousi, Nucl. Phys. B 584 (2000) 284.

[89] A. Sen, JHEP 0204 (2002) 048; JHEP 0207 (2002) 065; Mod. Phys. Lett. A 17 (2002) 1797.

[90] G.W. Gibbons, Phys. Lett. B 537 (2002) 1.

[91] S. Mukohyama, Phys. Rev. D 66 (2002) 024009.

[92] A. Frolov, L. Kofman and A. Starobinsky, Phys. Lett. B545 (2002) 8.

[93] T. Padmanabhan and T. Roy Choudhury, Phys. Rev. D 66 (2002) 081301.

[94] M. Sami, Phys. Rev. D 66 (2002) 043530.

[95] J.S. Bagla, H.K. Jassal and T. Padmanabhan, Phys. Rev. D 67 (2003) 063504.

[96] A. Feinstein, Phys. Rev. D 66 (2002) 063511.

[97] M. Fairbairn and M.H.G. Tytgat, Phys. Lett. B 546 (2002) 1.

[98] M. Salti, Int. J. Theor. Phys. 52 (2013) 4583.

[99] C. Ozel, H. Kayhan and G.S. Khadekar, Ad. Stud. Theor. Phys. 4 (2010) 117.

[100] S.W. Allen, et al., Mon. Not. Roy. Astron. Soc. 353 (2004) 457.

[101] J.C. Fabris, S.V.B. Goncalves and P.E. de Souza, Gen. Rel. Gravit. 34 (2002) 53.

[102] S.-L. Cao, S. Li, H.-R. Yu and T.-J. Zhang, RAA (Research in Astronomy and Astrophysics) 18 (2018) 26.

[103] C. Zhang, et al., RAA (Research in Astronomy and Astrophysics) 14 (2014) 1221.

[104] J. Simon, L. Verde and R. Jimenez, Phys. Rev. D 71 (2005) 123001.

[105] M. Moresco, L. Verde, L. Pozzetti, R. Jimenez, and A. Cimatti, J. Cosmol. Astropart. Phys. 7 (2012) 053.

[106] E. Gaztañaga, A.Cabré and L. Hui, MNRAS 399 (2009) 1663.

[107] X. Xu, A. J. Cuesta, N. Padmanabhan, D. J. Eisenstein and C. K. McBride, MNRAS 431 (2013) 2834.

[108] M. Moresco, et al., J. Cosmol. Astropart. Phys. 5 (2016) 014.

[109] D. Stern, R. Jimenez, L. Verde, M. Kamionkowski and S.A. Stanford, JCAP 02 (2010) 008.

[110] R. Jimenez, L. Verde, T. Treu and D. Stern, Astrophys. J. 593 (2003) 622.

[111] L. Samushia, et al., MNRAS 429 (2013) 1514.

[112] C. Blake, et al., MNRAS 425 (2012) 405.

[113] O. Farooq and B. Ratra, Astrophys. J. 766 (2013) L7.

[114] P. Thakur, S. Ghose and B.C. Paul, Mon. Not. R. Astron. Soc. 397 (2009) 1935.

[115] T. Delubac, et al., A&A 574 (2015) A59.

[116] W. Zimdahl, D. Pavon and L.P. Chimento, Phys. Lett. B 521 (2001) 133.

[117] V. Sahni, T.D. Saini, A.A. Starobinsky and U. Alam, Mon. Not. Roy. Astron. Soc. 344 (2003) 1057.

[118] U. Alam, V. Sahni, T.D. Saini and A.A. Starobinsky, MNRAS 344 (2003) 1057.

[119] X. Zhang, Int. J. Mod. Phys.D 14 (2005) 1597.

[120] M. R. Setare, J. Zhang and X. Zhang, J. Cosmol. Astropart. Phys. 3 (2007) 007.

[121] Z.-L. Yi and T.-J. Zhang, Phys. Rev. D 75 (2007) 083515.

[122] U. Debnath and M. Jamil, Astrophys. Space Sci. 335 (2011) 545.

[123] N.I. Jain, S.S. Bhoga and G.S. Khadekar, Int. J. Theor. Phys. 52 (2013) 4416.

[124] O. Bertolami, F. Gil Pedro and M. Le Delliou, Phys. Lett. B 654 (2007) 165.

[125] M. Jamil and M.A. Rashid, Eur. Phys. J. C 58 (2008) 111.

[126] E. Poisson and W. Israel, Phys. Rev. D 41 (1990) 1796.

[127] S.A. Hayward, Phys. Rev. D 53 (1996) 1938.

[128] Y.G. Gong and A. Wang, Phys. Rev. Lett. 99 (2007) 211301.

[129] G. Izquierdo and D. Pavon, Phys. Lett. B 633 (2006) 420.